

# Synthesis, Structural and Dielectric Studies of Nickel Substituted Cobalt-Zinc Ferrite

Gangatharan Sathishkumar<sup>1</sup>, Chidambaram Venkataraju<sup>2</sup>, Kandasamy Sivakumar<sup>3</sup>

<sup>1</sup>Department of Physics, Sri Sairam Engineering College, Chennai, India; <sup>2</sup>Department of Physics, A.M.A. College of Engineering, Kancheepuram, India; <sup>3</sup>Department of Physics, Anna University, Chennai, India.  
Email: sathishkumar.phy@ssec.edu.in

Received January 18<sup>th</sup>, 2010; revised January 25<sup>th</sup>, 2010; accepted February 1<sup>st</sup>, 2010.

## ABSTRACT

Nano particles of  $\text{Co}_{(0.5-x)}\text{Ni}_x\text{Zn}_{0.5}\text{Fe}_2\text{O}_4$  ( $x = 0$  to 0.3) is prepared by co-precipitation method. The X-ray diffraction analysis indicates the formation of single phase ferrite particle in nano size. The lattice constant for  $\text{Co}_{0.5}\text{Zn}_{0.5}\text{Fe}_2\text{O}_4$  is found to be 8.38 Å, but the lattice constant decreases when cobalt is replaced by nickel up to  $x = 0.2$  content. The formation of  $\text{Fe}^{2+}$  in octahedral site increases the lattice constant for the concentration  $x = 0.3$ . The dielectric constant of  $\text{Co}_{0.5}\text{Zn}_{0.5}\text{Fe}_2\text{O}_4$  is found to be less than the bulk sample. The migration of  $\text{Fe}^{3+}$  ion from octahedral site to tetrahedral site decreases the dielectric constant with increase in nickel concentration. The charge libration and electron hopping together form the basis for the conduction mechanism in this present compound.

**Keywords:** Magnetic Materials, Chemical Synthesis, X-ray Diffraction, Dielectric Properties

## 1. Introduction

Ferrites are good dielectric materials having low conductivity and have wide applications in the field of microwave devices. Nano crystalline ferrites are technologically important materials because of their unique electric, dielectric, magnetic and optical properties, which makes them suitable for many technological applications like microwave devices, transformers, electric generators, storage devices etc. [1]. When Co-Zn ferrites are subjected to alternating magnetic field it shows low energy loss [2]. Many studies on Co-Zn ferrites in the bulk crystalline form were prepared by usual ceramic technique [3, 4]. Ram Kripal Sharma has reported the synthesis of chromium substituted nano particles of cobalt zinc ferrites by coprecipitation method [5]. A. Tawfik has reported the electro mechanical properties of  $\text{Co}_{0.6}\text{Zn}_{0.4}\text{Fe}_2\text{O}_4$  ferrite transducer [6]. Josyulu [7] have studied the dielectric behavior for Co-Zn, and Mg-Zn ferrites as a function of temperature and frequency, Sonal Signaj has reported preparation and characterization of nano sized nickel substituted cobalt ferrite [8]. Gul *et al.* [9] have prepared nanoparticles of  $\text{Co}_{1-x}\text{Zn}_x\text{Fe}_2\text{O}_4$  with stoichiometric proportion ( $x$ ) varying from 0.0 to 0.6 by the chemical coprecipitation method. In the present investigation the studies on nano particles of  $\text{Co}_{(0.5-x)}\text{Ni}_x\text{Zn}_{0.5}\text{Fe}_2\text{O}_4$  ( $x = 0$  to 0.3), synthesized by chemical co-precipitation method is reported.

## 2. Experimental Details

Nano particles of  $\text{Co}_{(0.5-x)}\text{Ni}_x\text{Zn}_{0.5}\text{Fe}_2\text{O}_4$  with  $x$ - varying from  $x = 0.0$  to 0.3 were prepared by coprecipitation method. Aqueous solution of  $\text{FeCl}_3$ ,  $\text{ZnSO}_4 \cdot 7\text{H}_2\text{O}$ ,  $\text{CoCl}_2 \cdot 6\text{H}_2\text{O}$  and  $\text{NiCl}_2 \cdot 6\text{H}_2\text{O}$  in the respective stoichiometry (100 ml of solution containing (0.5- $x$ ) M  $\text{CoCl}_2$ , ( $x$ ) M  $\text{NiCl}_2$ , 0.5 M  $\text{ZnSO}_4$  and 100 ml of 2 M  $\text{FeCl}_3$ ) were mixed thoroughly using magnetic stirrer at 80°C. It is then transferred immediately into a boiling solution of NaOH (0.55 M dissolved in 1330 ml of distilled water) under constant stirring and a pH of 12 is maintained throughout the reaction. Conversion of metal salts into hydroxides and subsequent transformation of metal hydroxide into nanoferrites takes place upon 100°C and maintained for 60 minutes until the reaction is complete. The nanoferrites thus formed were isolated by centrifugation and washed several times with deionized water followed by acetone and then dried at room temperature. The dried powder is grounded thoroughly in a clean agate mortar and then the material is pelletized at 5 ton pressure for about 3 min. The pellet and the powder were sintered at 500°C in a furnace for about 2 hrs.

XRD measurement is done for the sample by PAN analytical X'pert PRO diffractometer using  $\text{Cu K}_\alpha$  radiation (operated at 45 kV and 40 mA) source. Data collection is done for every 10 sec at every 0.02° in the range

20° to 80° in 2 $\theta$ .

TEM analysis is done using High-resolution transmission electron microscopy (HRTEM) JEOL 3010, 300 kV instrument with UHR pole piece for the sample  $x = 0.2$ .

The dielectric studies for the pelletized sample were carried out between the temperatures 40°C to 550°C in the frequency range 50 Hz to 10 MHz using HIOKI 3532-50 LCR HiTester. The Dielectric constant is measured using the relation,  $\epsilon^1 = Cd/\epsilon_0 A$ , where C is the capacitance of the sample in Farad, d and A are the thickness and area of the flat surface of the pellet and  $\epsilon_0$  the constant of permittivity of the free space. Dielectric Loss is calculated using the relation  $\tan(\delta) = D$  and ac-conductivity using the relation  $\sigma_{ac} = \epsilon^1 \epsilon_0 \omega \tan(\delta)$ .

### 3. Result and Discussion

#### 3.1 XRD Analysis

Figure 1 shows the X-ray diffraction pattern of  $\text{Co}_{(0.5-x)}\text{Ni}_x\text{Zn}_{0.5}\text{Fe}_2\text{O}_4$  (with  $x = 0$  to 0.3), it shows the formation of spinel ferrite phase in all the samples. The interplanar distance  $d$  (Å) are calculated using Bragg's law. The broad XRD line indicates that the ferrites particles are in nanosize. All the peaks in the diffraction pattern have been indexed and the refinement of the lattice parameter was done using PowderX software. The crystalline size for each composition are calculated from XRD line width of the (311) peak using Scherrer formula [10]. The values of the particle size, lattice constant measured density  $\rho_m$  and the X-ray density  $\rho_x$  as deduced from the X-ray data are given by Table 1.

The measured density,  $\rho_m$  is determined using the formula  $\rho_m = m/(r^2 h)$ , where  $m$  is the mass,  $r$  the radius and  $h$  the height of the sample. The X-ray density of the prepared samples is calculated by the relation  $\rho_x = 8 M/ N a^3$ , where  $M$  is the molecular weight of the samples,  $N$  is the Avogadro's number and 'a' is the lattice constant.

The lattice constant for  $\text{Co}_{0.5}\text{Zn}_{0.5}\text{Fe}_2\text{O}_4$  in the present investigation is 8.38 Å. This is similar to the values reported by P. B. Pandya *et al.*, and Ana Maria Rangel de Figuerido Teixeira *et al.* [11,12]. The lattice constant decreases with the increase in Ni concentration up to  $x = 0.2$ . This can be explained on the basis of cation stoichiometry. The ionic radius of  $\text{Ni}^{2+}$  ions (0.69 Å) is smaller than the ionic radius of  $\text{Co}^{2+}$  cations (0.72 Å) and hence the

replacement of Cobalt by Ni in  $\text{Ni}_x\text{Co}_{(0.5-x)}\text{Zn}_{0.5}\text{Fe}_2\text{O}_4$  causes a decrease in lattice constant obeying Vegard's law. The increase in lattice constant for the value  $x = 0.3$  may be due to the possible presence or formation of  $\text{Fe}^{2+}$  in the octahedral sites. Since ionic radius of  $\text{Fe}^{2+}$  (0.74 Å) ion is larger than  $\text{Fe}^{3+}$  ion (0.64 Å), the lattice constant increases. The intensities of the (220) and (440) planes are more sensitive to cations in tetrahedral and octahedral sites respectively [13,14].  $\text{Ni}^{2+}$  and  $\text{Co}^{2+}$  ion prefers octahedral sites whereas  $\text{Fe}^{3+}$  ions prefer both tetrahedral and octahedral sites. When the particle size reduces to nano dimension there is change in cation distribution [8]  $\text{Co}^{2+}$  ion occupies both tetrahedral and octahedral sites. From Table 2 it is clear that the intensity of (440) decreases with increase in  $\text{Ni}^{2+}$  concentration. This is explained due to the decrease in  $\text{Co}^{2+}$  ion in octahedral site with the increase in  $\text{Ni}^{2+}$  concentration.

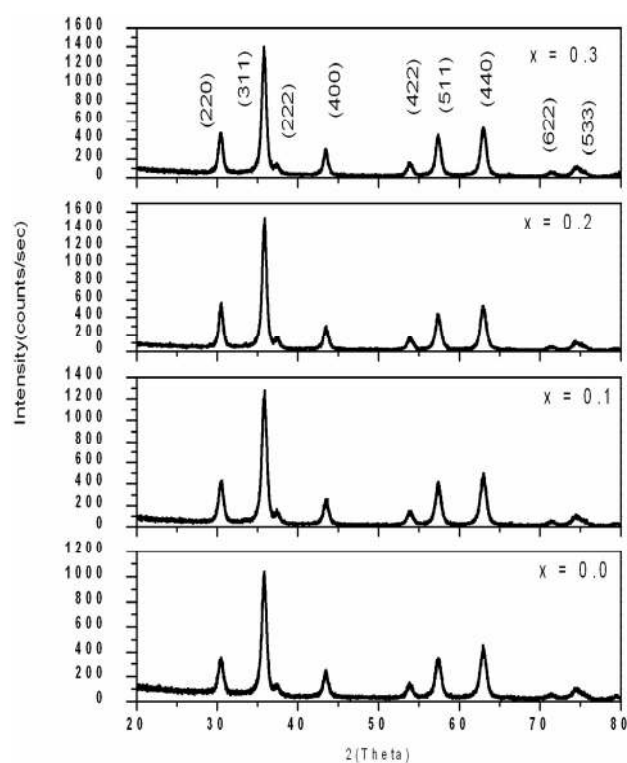


Figure 1. XRD pattern for the system  $\text{Co}_{(0.5-x)}\text{Ni}_x\text{Zn}_{0.5}\text{Fe}_2\text{O}_4$  ( $x = 0$  to 0.3)

Table 1. Structural parameters of  $\text{Ni}_x\text{Co}_{(0.5-x)}\text{Zn}_{0.5}\text{Fe}_2\text{O}_4$  sintered at 500°C

Composition	Particle size 't' (nm)	Lattice constant 'a' (Å)	X-ray density $\rho_x$ (gm/cm <sup>3</sup> )	Measured density $\rho_m$ (gm/cm <sup>3</sup> )	Porosity 'P'
x = 0.0	10.75	8.3778	5.3742	2.182	0.5944
x = 0.1	10.99	8.3555	5.4163	2.155	0.6022
x = 0.2	12.24	8.3429	5.4393	2.117	0.6108
x = 0.3	11.86	8.3496	5.4257	2.125	0.6083

**Table 2. Comparison of X-ray intensity**

Composition	I(220)	I(440)
x = 0.0	34.2	35
x = 0.1	34.28	30.97
x = 0.2	35.61	27.02
x = 0.3	34.71	31.17

The increase in intensity of (220) plane may be due to the migration of  $\text{Fe}^{3+}$  ion from octahedral site to tetrahedral site, as  $\text{Co}^{2+}$  ion is replaced by nickel. The intensities are found to reverse for the concentration  $x = 0.3$ . This may be due the presence of  $\text{Fe}^{2+}$  ion in the octahedral site formed due to reduction of  $\text{Fe}^{3+}$  ions to  $\text{Fe}^{2+}$  ions for higher nickel concentration.

### 3.2 Transmission Electron Microscopy Analysis

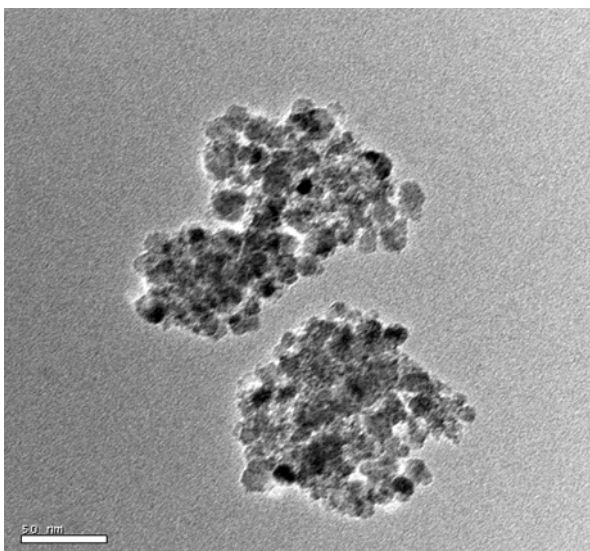
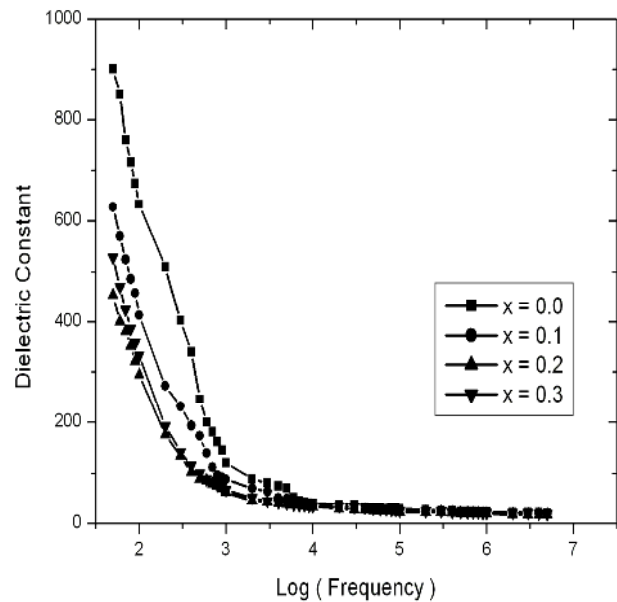
The particle size and morphology of the sample with  $x = 0.2$  is shown in the **Figure 2**. The average particle size is around 15 nm.

TEM analysis revealed that the particles are nearly spherical. The particle size determined from TEM was found to be in close agreement with that obtained from XRD studies.

### 3.3 Dielectric Properties

#### 3.3.1 Dielectric Constant

The variation in dielectric constant ( $\epsilon'$ ) with frequency at room temperature for the samples  $\text{Co}_{(0.5-x)}\text{Ni}_x\text{Zn}_{0.5}\text{Fe}_2\text{O}_4$  with  $x = 0.0, 0.1, 0.2$  and  $0.3$  is shown in **Figure 3**. The dielectric constant is found to be less than bulk sample for a frequency of 100 KHz at room temperature. The dielectric constant for bulk  $\text{Co}_{0.5}\text{Zn}_{0.5}\text{Fe}_2\text{O}_4$  as reported

**Figure 2. TEM image of  $\text{Co}_{0.3}\text{Ni}_{0.2}\text{Zn}_{0.5}\text{Fe}_2\text{O}_4$** **Figure 3. Effect of frequency on dielectric constant ( $\epsilon'$ ) at room temperature  $\text{Co}_{(0.5-x)}\text{Ni}_x\text{Zn}_{0.5}\text{Fe}_2\text{O}_4$** 

by M. A. Ahmed [15] is 105, whereas in the present investigation the dielectric constant for  $\text{Co}_{0.5}\text{Zn}_{0.5}\text{Fe}_2\text{O}_4$  with particle size 10 nm is calculated as 28. This low dielectric loss is attributed to homogeneity, better symmetry and small grain size when compared with bulk sample [16]. Small grains have large surface boundaries and are the regions of high resistance, this reduces the interfacial polarization. From **Figure 3** it is clear that the dielectric constant decreases with increase in frequency, showing dispersion in low frequency range. All samples show dispersion due to Maxwell-Wagner [17,18] and are also in agreement with the Koop's phenomenological theory [19]. The decrease in dielectric constant at higher frequency can be explained on the basis that the solid is assumed as composed of well conducting grains and is separated by non conducting grain boundaries, when electrons reach such non conducting grain boundaries through hopping the resistance of the grain boundary is high, hence the electron pile up at the grain boundaries and produce polarization. At higher frequency beyond a particular limit, the electron does not follow the alternating field. This decreases the probability of electrons reaching the grain boundary and as result polarization decreases [17,19]. The decrease in dielectric constant with increase in nickel concentration may be due to the migration of  $\text{Fe}^{3+}$  ions from octahedral site to tetrahedral site.

This decreases the hopping and hence decreases the polarization up to  $x = 0.2$ . The increase in dielectric constant for the concentration  $x = 0.3$  may be due to the formation of  $\text{Fe}^{2+}$  ions in octahedral site. The increase in  $\text{Fe}^{2+}$  ions in octahedral site increases the hopping between  $\text{Fe}^{2+}$  and  $\text{Fe}^{3+}$  and hence increases the polarization.

This results in the local displacement of electrons in the direction of applied field thereby increasing the dielectric constant.

**Figure 4** shows the variation of dielectric constant at 1 MHz with temperature for mixed  $\text{Co}_{(0.5-x)}\text{Ni}_x\text{Zn}_{0.5}\text{Fe}_2\text{O}_4$  (where  $x = 0.0$  to 0.3). The dielectric constant increases gradually with increase in temperature up to a certain temperature designated as dielectric transition temperature ( $T_d$ ). However beyond this temperature, the values of the dielectric constant were found to decrease continuously.

A similar temperature variation of the dielectric constant has been reported by D. Ravindra and K. Vijayakumar [20], Olofa [21]. This change in the dielectric behavior beyond transition temperature may be due a magnetic transition from ferromagnetic to paramagnetic. The increase in the dielectric constant with temperature can be explained on the basis that as the temperature increases the hopping between  $\text{Fe}^{2+}$  and  $\text{Fe}^{3+}$  ions on the octahedral sites is thermally activated this electron hopping causes local displacement in the direction of the external applied field and as a result the dielectric polarization increases. Therefore the dielectric constant increases. However beyond the transition temperature, the ions and electrons are less oriented towards the field direction and hence the dielectric constant decreases.

### 3.3.2 Dielectric Loss

**Figure 5** shows the variation of dielectric loss tangent  $\tan(\delta)$  with frequency at room temperature in all the cases there is decrease in dielectric loss initially followed by resonance peak with increase in frequency. The appearance of a resonance peak can be explained as follows. If an ion has more than one equilibrium position, say two positions  $A$  and  $B$ , of equal potential energies, separated by a potential barrier, the probabilities of jumping of ions from  $A$  to  $B$  and from  $B$  to  $A$  are the same. Depending upon this probability, the ion exchanges position between the two states with some frequency, called the natural frequency of jump between the two positions. When an external alternating electric field of the same frequency is applied, maximum electrical energy is transferred to the oscillating ions and power loss shoots up, thereby resulting in resonance according to Debye relaxation theory [22].

The loss peak occurs when the applied field is in phase with the dielectric and the condition  $\omega\tau = 1$  is satisfied, where  $\omega = 2\pi f$ ,  $f$  being the frequency of the applied field and  $\tau$  the relaxation time is related to jumping probability per unit time  $p$ , by an equation  $\tau = p/2$  or  $f_{\max} \propto p$ . Now an increase in  $f_{\max}$  with increasing Nickel content indicates the hopping or jumping probability per unit time increases. The shifting of relaxation peak towards higher frequency side is due to increase in nickel concentration since nickel prefers B-site which strengthens the dipole-dipole interaction leading to hindrance to the rotation of the dipoles [23].

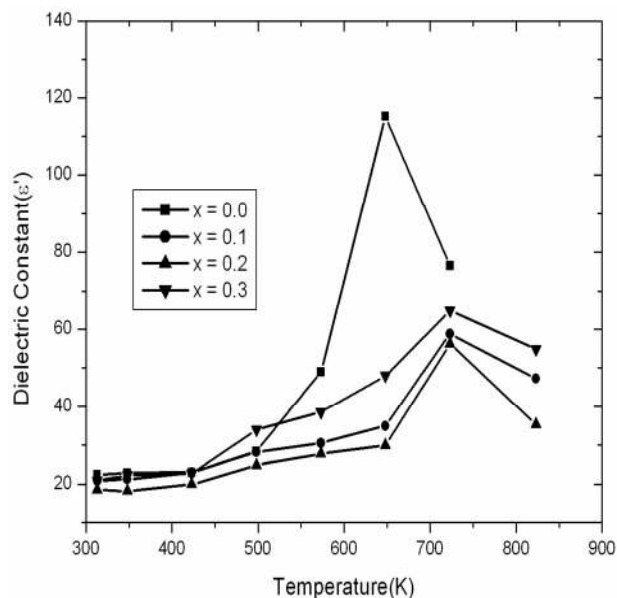


**Figure 4.** Variation of dielectric constant ( $\epsilon'$ ) with temperature at 1 MHz for  $\text{Co}_{(0.5-x)}\text{Ni}_x\text{Zn}_{0.5}\text{Fe}_2\text{O}_4$

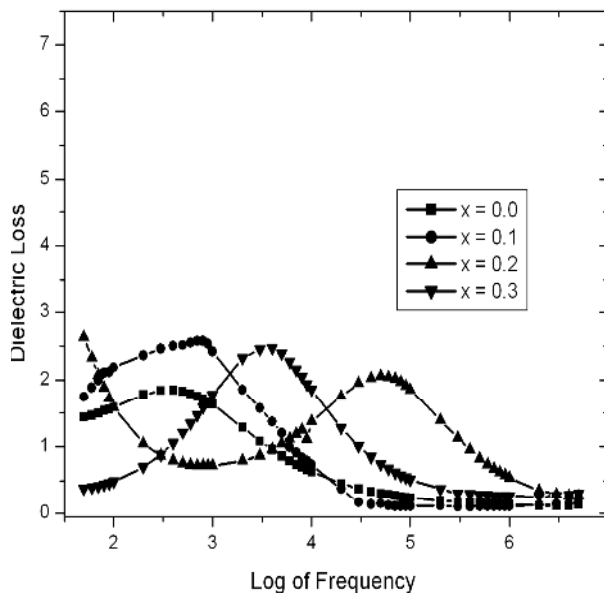


**Figure 5** Plot of dielectric loss tangent with frequency for  $\text{Co}_{(0.5-x)}\text{Ni}_x\text{Zn}_{0.5}\text{Fe}_2\text{O}_4$

### 3.3.3. A C Conductivity

**Figure 6** shows the variation of ac conductivity ( $\log\sigma$ ) with frequency at 300 K. The entire sample shows increase in conductivity with increase in frequency, which is the normal behavior of ferrites. The conduction mechanism in ferrites can be explained on the basis of hopping of charge carriers between  $\text{Fe}^{2+}$  -  $\text{Fe}^{3+}$  ions on octahedral sites.

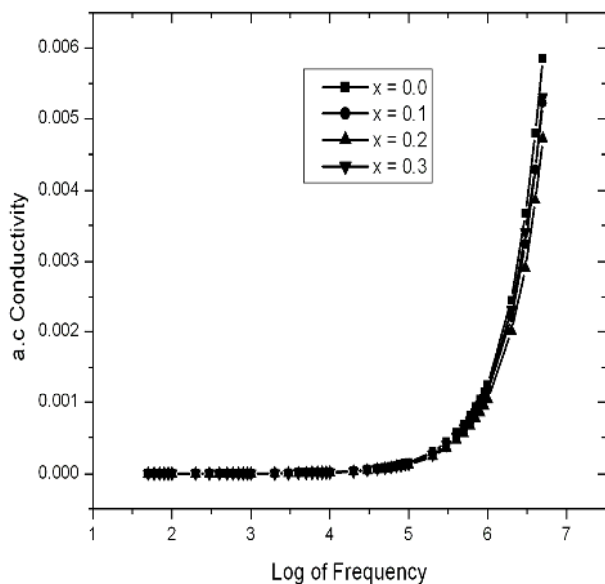


Figure 6. Plot of AC conductivity  $\sigma$  with frequency  $\text{Co}_{(0.5-x)}\text{Ni}_x\text{Zn}_{0.5}\text{Fe}_2\text{O}_4$

#### 4. Conclusions

The ferrite phase  $\text{Co}_{(0.5-x)}\text{Ni}_x\text{Zn}_{0.5}\text{Fe}_2\text{O}_4$  ( $x = 0$  to  $0.3$ ) is prepared by co-precipitation technique. The ferrite phase formation is confirmed by XRD studies. The particle size is found to be 12 nm by XRD calculation, which is in close agreement with the TEM result 15 nm. For nickel content  $x = 0.0$  to  $0.2$  there is a migration of  $\text{Fe}^{3+}$  ions from octahedral site to tetrahedral site. For  $x = 0.3$  there is a formation of  $\text{Fe}^{2+}$  ion in the tetrahedral site due to reduction of  $\text{Fe}^{3+}$  ions to  $\text{Fe}^{2+}$  ions for higher nickel content. This results in an increase in the lattice constant as calculated from XRD analysis. Dielectric constant is found to decrease with Ni content up to  $x = 0.2$  and increases for nickel content  $x = 0.3$ . The charge libration and electron hopping together form the basis for the conduction mechanism in  $\text{Co}_{(0.5-x)}\text{Ni}_x\text{Zn}_{0.5}\text{Fe}_2\text{O}_4$  ( $x = 0$  to  $0.3$ ) ferrites.

#### REFERENCES

- [1] S. Gubbala, H. Nathani, K. Koziol and R. D. K. Misra, "Magnetic Properties of Nanocrystalline Ni-Zn, Zn-Mn, and Ni-Mn Ferrites Synthesized by Reverse Micelle Technique," *Physica B: Condensed Matter*, Vol. 348, No. 1-4, 2004, pp. 317-328.
- [2] R. Arulmurugan, G. Vaidyanathan, S. Senthilnathan and B. Jeyadevan, "Co-Zn Ferrite Nanoparticles for Ferrofluid Preparation: Study on Magnetic Properties," *Physica B: Condensed Matter*, Vol. 363, No. 1-4, 2005, pp. 225-231.
- [3] M. U. Islam, M. U. Rana and Abbas, "Study of Magnetic Interactions in Co-Zn-Fe-O System," *Materials Chemistry and Physics*, Vol. 57, 1998, pp. 190-193.
- [4] O. M. Hemedat and M. I. Abd El-Ati, "Spectral Studies of  $\text{Co}_{0.6}\text{Zn}_{0.4}\text{Fe}_2\text{O}_4$  at Different Soaking Times," *Materials Letters*, Vol. 51, No. 1, 2001, pp. 42-47.
- [5] R. K. Sharma, O. Suwalka, N. Lakshmi, K. Venugopala, A. Banerjee and P. A. Joy, "Synthesis of Chromium Substituted Nano Particles of Cobalt Zinc Ferrites by Coprecipitation," *Materials Letters*, Vol. 59, 2005, pp. 3402-3405.
- [6] A. Tawfik, "Electromechanical Properties of  $\text{Co}_{0.6}\text{Zn}_{0.4}\text{Fe}_2\text{O}_4$  Ferrite Transducer," *Journal of Magnetism and Magnetic Materials*, Vol. 237, No. 3, 2001, pp. 283-287.
- [7] O. S. Josyulu and Sobhanadri, "DC Conductivity and Dielectric Behaviour of Cobalt-Zinc Ferrites," *Physica Status Solidi (a)*, Vol. 59, 1980, pp. 323-329.
- [8] Singhal, J. Singh, S. K. Barthwal and K. Chandra, "Preparation and Characterisation of Nanosize Nickel-Substituted Cobalt Ferrites  $\text{Co}_{(1-x)}\text{Ni}_x\text{Fe}_2\text{O}_4$ ," *Journal of Solid State Chemistry*, Vol. 178, No. 10, 2005, pp. 3183-3189.
- [9] I. H. Gul, A. Z. Abbasi, F. Amin, M. Anis-Ur-Rehman and A. Maqsood, "Structural, Magnetic and Electrical Properties of  $\text{Co}_{1-x}\text{Zn}_x\text{Fe}_2\text{O}_4$  Synthesized by Co-precipitation Method," *Journal of Magnetism and Magnetic Materials*, Vol. 311, No. 2, 2007, pp. 494-499.
- [10] B. Cullity, "Elements of X-Ray Diffraction," Addison-Wesley, London, 1978.
- [11] P. B. Pandya, H. H. Joshi and R. G. Kulkarni, "Bulk Magnetic Properties of Co-Zn Ferrite Prepared by Co-precipitation Method," *Journal of Materials Science*, Vol. 26, 1991, pp. 5509-5512.
- [12] A. M. R. de Figueiredo Teixeira, T. Ogasawara and M. C. de Souza Nobrega, "Investigation of Sintered Cobalt-Zinc Ferrite Synthesized by Co-precipitation at different Temperatures. A Relation between Microstructure and Hysteresis Curve," *Materials Research*, Vol. 9, No. 3, 2006, pp. 257-262.
- [13] B. P. Ladgaonkar and A. S. Vaingankar, "X-ray Diffraction Investigation of Cation Distribution in  $\text{Cd}_x\text{Cu}_{(1-x)}\text{Fe}_2\text{O}_4$ ," *Materials Chemistry and Physics*, Vol. 56, No. 3, 1998, pp. 280-283.
- [14] C. S. Narasimhan and C. S. Swamy, "Studies on the Solid State Properties of the Solid Solution Systems  $\text{MgAl}_{(2-x)}\text{Fe}_x\text{O}_4$ ," *Physica Status Solidi (a)*, Vol. 59, 1980, p. 817.
- [15] M. A. Ahmed, K. A. Darwish, H. Mikhail, M. Mounir and E. H. El-Khawas, "Effect of Cation Concentration on the Relaxation Phenomena of Co-Zn Ferrite," *Physica Scripta*, Vol. 55, 1997, pp. 750-755.
- [16] P. Mathur, A. Thakur and M. Singh, "Effect of Particle Size on the Properties of Mn-Zn-In Ferrites," *Physica Scripta*, Vol. 77, 2008.
- [17] J. C. Maxwell, "A Treatise on Electricity and Magnetism," Oxford University Press, New York, Vol. 1, 1973, p. 828.
- [18] K. W. Wagner, "Zur Theorie der Unvollkommenen Dielektrika," *Annalen der Physik*, Vol. 40, 1913, pp. 817-855.

- [19] C. G. Koops, "On the Dispersion of Resistivity and Dielectric Constant of Some Semiconductors at Audio-frequencies," *Physical Review*, Vol. 83, 1951, p.121.
- [20] D. Ravinder and V. kumar, "Dielectric Behaviour of Erbium Substituted Mn-Zn Ferrites," *Bulletin of Materials Science*, Vol. 24, No. 5, 2001, pp. 505-509.
- [21] S. A. Olofa, "Oscillographic Study of the Dielectric Polarization of Cu-doped NiZn Ferrite," *Journal of Magnetism and Magnetic Materials*, Vol. 131, 1994, pp. 103-106.
- [22] U. N. Trivedi, M. C. Chhantbar, K. B. Modi and H. H. Johi, "Frequency Dependant Dielectric Behaviour of Cadmium and Chromium, Co-substituted Nickel Ferrite," *Indian Journal of Pure and Applied Physics*, Vol. 43, 2005, pp. 688-690.
- [23] K. Amarendra, T. Singh, C. Goel and R. G. Mendiratta, "Dielectric Properties of Mn-Substituted Ni-Zn Ferrite," *Journal of Applied Physics*, Vol. 91, No. 10, 2002, p. 6626.